# *In vivo* sequential mutagenesis in germinal center B cells using a dual-recombinase approach: FOXO1 re-expression upon FOXO1 knockout rescues class switch recombination

Carlota Farré Díaz[1,2,3,4,#], Eleni Kabrani[1,5,#], Wiebke Winkler[1,2,3,4], Claudia Salomon[1], F. Thomas Wunderlich[6,7,8], Martin Janz[2,3,4] and Klaus Rajewsky[1]

[1]Immune Regulation and Cancer, Max Delbrück Center for Molecular Medicine in the Helmholtz Association, Berlin 13125, Germany.

[2]Biology of Malignant Lymphomas, Max Delbrück Center for Molecular Medicine in the Helmholtz Association, Berlin 13125, Germany.

[3]Experimental and Clinical Research Center, a cooperation between the Max Delbrück Center for Molecular Medicine in the Helmholtz Association and the Charité – Universitätsmedizin Berlin, Berlin 13125, Germany.

[4]Hematology, Oncology and Cancer Immunology, Charité – Universitätsmedizin Berlin, Berlin 13125, Germany.

[5]Genome Diversification & Integrity, Max Delbrück Center for Molecular Medicine in the Helmholtz Association, Berlin 13125, Germany.

[6]Faculty of Medicine and University Hospital Cologne, Center for Molecular Medicine Cologne (CMMC), University of Cologne, Cologne 50931, Germany

[7]Cologne Excellence Cluster for Stress Responses in Ageing-Associated Diseases (CECAD), University of Cologne, Cologne 50931, Germany.

[8]Max-Planck-Institute for Metabolism Research, Cologne 50931, Germany

[#] These authors contributed equally

Corresponding author: Klaus Rajewsky, Max-Delbrück-Center, Robert-Rössle-Straße 10, 13125 Berlin-Buch, klaus.rajewsky@mdc-berlin.de

Keywords: germinal center, sequential mutagenesis, dual-recombinase, Cre, Dre

Abbreviations: **4-OHT:** 4-hydroxytamoxifen, **BFP:** blue fluorescent protein, **Cγ1:** immunoglobulin heavy constant gamma 1, **CSR:** class switch recombination, **DZ:** dark zone, **GC:** germinal center, **GCBC**: GC B cell; **KO:** knockout, **LZ:** light zone, **MBC**: memory B cell, **NP-CGG**: 4-hydroxy-3-nitrophenylacetyl-conjugated chicken gamma globulin, **PC**: plasma cell, **R26:** Rosa 26, **SHM:** somatic hypermutation, **TAM:** tamoxifen.

## Abstract

Modeling complex (patho)physiological processes by sequential mutagenesis in mice is limited by the lack of optimized genetic tools and complex breeding strategies. We present a new Cre/DreERT2 dual-recombinase germinal center B-cell (GCBC)-specific strain, with co-expression of the recombinases from a single allele. This enables highly efficient Cre-mediated FOXO1 knockout followed by time-controlled, efficient Dre-mediated FOXO1 re-expression and functional rescue in GCBCs, demonstrating suitability for precise targeted sequential mutagenesis *in vivo*.

Site-specific recombination systems, such as Cre/loxP, are key technologies to study gene function and (patho)physiological processes *in vivo*. Dual-recombinase approaches represent a further technical development that enables more precise disease modelling, in particular with respect to multistep genetic manipulations and lineage tracing[1,2]. However, one limitation of the currently available systems is that recombinases are expressed from different loci, hereby requiring the generation of complex compound mutant mice – containing separate transgenes encoding the recombinases together with the respective target alleles – and thus complicating the analysis both in terms of breeding time frame and fidelity of sequential mutagenesis at the level of individual cells. Here, we describe a dual-recombinase mouse strain in the context of germinal center (GC) B cells (GCBCs), where Cre and the tamoxifen (TAM)-dependent DreERT2 recombinases are co-expressed from the immunoglobulin heavy constant gamma 1 (*Ighg1/Cγ1*) locus and thus at the initiation of the GC response. By sequentially targeting the endogenous *Foxo1* locus during the GCBC reaction as a proof-of-concept experiment, we demonstrate highly efficient Cre-mediated FOXO1 knockout (KO) with perturbation of GC physiology, followed by time-controlled Dre-mediated FOXO1 re-expression and phenotypic rescue, demonstrating that this system can be used *in vivo* as a genetic recombination switch that is precisely controlled with respect to cellular compartment and time.

Upon antigen encounter, mature B cells undergo clonal expansion in distinct histological structures called GCs. During the early phases of GC formation, activated B cells diversify their immunoglobulin repertoire via class switch recombination (CSR), and later, in the course of the GC reaction, via somatic hypermutation (SHM) of antibody V region genes[3]. Positively selected GCBCs differentiate into memory B cells (MBCs) or antibody-secreting plasma cells (PCs), thus shaping the humoral immune response[3]. Both CSR and SHM require the introduction and the efficient repair of DNA strand breaks in the immunoglobulin loci[4]. Errors during these processes can lead to oncogenic mutations and/or translocations, rendering (post)-GCBCs the origin of most B cell malignancies[5]. In order to study the physiology and malignant transformation of GCBCs, a number of Cre mouse lines have been generated[6,7,8,9,10]. However, none of the currently available lines allows for the genetic manipulation of GCBC differentiation in a stepwise fashion. This technical limitation prevents not only the *in vivo* investigation of the role and cooperation of genes at different time points during the GC reaction, but also the study of the sequential acquisition of oncogenic events in this microenvironment, underlying malignant transformation.

69 Addressing this experimental challenge, we have generated a novel dual-recombinase
70 GCBC-specific mouse strain, in which Cre and the TAM-inducible DreERT2
71 recombinases are concomitantly expressed from the *Ighg1/Cγ1* locus, hereafter called
72 the *Cγ1-CDE* strain (Fig. 1A). *Cγ1* encodes the constant region of IgG1. Upon T cell-
73 dependent immunization, most activated B cells that enter the GC produce germline ɣ1
74 transcripts in response to IL4[6], allowing the expression of both recombinases – and thus
75 Cre activity – from the *Cγ1* locus early on. Cells that have completed switch
76 recombination to IgG1 continue to express the recombinases during the course of the
77 GC reaction. Since DreERT2 activation is dependent on TAM administration, the second
78 (Dre-mediated) recombination event can be induced in a time-controlled manner,
79 selectively in cells having undergone Cre induction. To functionally validate the newly
80 generated strain, *Cγ1-CDE* mice were crossed to the fluorescent reporter strains *Rosa*
81 *26 (R26)-BFP*$^{stopF}$[11] and *R26-ZsGreen*$^{stopRox}$[12] for detection of Cre- and Dre-mediated
82 recombination, respectively. *Cγ1-CDE*, *R26-BFP*$^{stopF}$, *R26-ZsGreen*$^{stopRox}$ compound
83 mutant mice were immunized with NP-CGG and TAM was administered at days 2-5, 9-
84 12 or 15-18 after immunization with subsequent flow cytometric analysis at days 7, 14 or
85 21, respectively (Fig. 1B-G). Consistent with the previous characterization of the *Cγ1-*
86 *Cre* allele[6], up to 96% of splenic GCBCs were labelled through Cre-mediated
87 recombination (BFP$^+$ GCBCs, Fig. 1B-D, Supplemental Fig.1A-B). Further gating on
88 these BFP$^+$ GCBCs showed a robust and highly efficient Dre-mediated recombination at
89 all time points analyzed (Fig. 1B-D), with the highest dual labelling efficiency on day 7 of
90 analysis (up to 60% ZsGreen$^+$ cells within the BFP$^+$ GCBC population, Fig. 1B). GCs are
91 organized into two phenotypically and functionally distinct compartments, the dark zone
92 (DZ) and the light zone (LZ)[3]. GCBCs in both compartments were successfully labeled
93 (Fig. 1E-G). Importantly, in the absence of TAM, no Dre recombination was detected,
94 demonstrating that Dre-mediated recombination is tightly controlled *in vivo* (Fig. 1E-G).

95 Germline ɣ1 transcripts are detected in the activated B cell pool early on upon
96 immunization, and their presence is independent of the subsequent IgG1 CSR event *per*
97 *se*[13,6]**.** Accordingly, Cre-mediated followed by Dre-mediated sequential mutagenesis is
98 achieved not only in IgG1$^+$ (up to 70% ZsGreen$^+$ within BFP$^+$ cells) but also in IgM$^+$ (up
99 to 42% ZsGreen$^+$ within BFP$^+$ cells) GCBCs in our mouse model at all three time points
100 analyzed (Supplemental Fig. 1E-F).

101 In addition, analysis of the post-GC compartments revealed the feasibility of labeling
102 these cell types as well. MBCs exhibited solid Cre-mediated and Dre-mediated
103 sequential mutagenesis (up to 84% BFP$^+$ cells and 60% ZsGreen$^+$ within BFP$^+$ cells, Fig.
104 1B-D, Supplemental Fig. 1C). Analysis of the splenic plasmablast/PC compartment (Fig.

105 1B-D, Supplemental Fig. 1C) exhibited the highest labelling efficiency for this
106 compartment at day 7 of analysis (up to 75% $BFP^+$ cells and 50% $ZsGreen^+$ within $BFP^+$
107 cells, Fig. 1B), indicating the feasibility to target and thus study extrafollicular PCs with
108 our *Cγ1-CDE* strain. However, the fraction of labelled PCs is reduced when analyzing
109 the immunized mice at later time points (day 14 and day 21, Fig. 1C-D), possibly due to
110 the short lifespan of extrafollicular PCs.

111 The FOXO1 transcription factor, although dispensable for GC
112 development/maintenance, positively regulates both GC compartmentalization (DZ
113 compartment) and CSR[14,15]. To this end, and as a proof-of-concept experiment, we
114 aimed at genetically manipulating the endogenous *Foxo1* locus in a sequential manner.
115 In addition to the already published Cre-inducible *Foxo1* null allele ($Foxo1^{fl}$)[16], we
116 generated a rox-controlled, Dre-inducible *Foxo1* allele ($Foxo1^{stopRox}$). The $Foxo1^{stopRox}$
117 allele carries a STOP cassette flanked by rox sites in front of the endogenous *Foxo1*
118 open reading frame, leading to the inactivation of the allele in the absence of Dre activity
119 (Supplemental Fig. 2A). Of note, while hemizygous *Foxo1* mice are viable and fertile,
120 homozygous germline deletion of FOXO1 results in embryonic lethality[17,18]. In order to
121 verify that the $Foxo1^{stopRox}$ allele is functional upon deletion of the STOP cassette, splenic
122 B cells from *Cγ1-CDE*, $Foxo1^{stopRox/wt}$ compound mutant mice were activated *in vitro* and
123 cultured in the presence or absence of 4-hydroxytamoxifen (4-OHT), followed by
124 sequencing analysis of *Foxo1* transcripts (Fig. 2A). Indeed, expression of the targeted
125 allele was observed solely in the presence of 4-OHT, demonstrating not only that the
126 $Foxo1^{stopRox}$ allele is functional, but also the tightness of the system. *In vivo*, crossing of
127 *Cγ1-CDE*, $Foxo1^{stopRox}$ mice with $Foxo1^{fl}$ transgenic mice (*Cγ1-CDE*, $Foxo1^{fl/stopRox}$) would
128 generate a scenario in which upon NP-CGG immunization, and therefore Cre activation,
129 the $Foxo1^{fl}$ allele would be deleted, resulting in a FOXO1-KO condition in GCBCs (Fig.
130 2B). GCBC-specific FOXO1 deletion is expected to lead to loss of the DZ compartment
131 and to defects in CSR, while maintaining the GCBC phenotype[11,12]. In a second step
132 upon TAM treatment – and hence Dre nuclear translocation and activation –, re-
133 expression of FOXO1 would be achieved from the $Foxo1^{stopRox}$ allele, thus leading to a
134 rescue of the previously induced FOXO1 deficiency (Fig. 2B). To address whether the
135 sequential deletion and re-activation of FOXO1 from the endogenous locus could restore
136 GC compartmentalization and CSR, experimental *Cγ1-CDE*, $Foxo1^{fl/stopRox}$, *R26-*
137 $ZsGreen^{stopRox}$ (in short $Foxo1^{fl/stopRox}$) and control *Cγ1-CDE*, $Foxo1^{fl/wt}$, *R26-*
138 $ZsGreen^{stopRox}$ (in short $Foxo1^{fl/wt}$) mice were immunized with NP-CGG, subsequently
139 treated with TAM (day 10-12 after immunization) and analyzed on day 14. The *R26-*
140 $ZsGreen^{stopRox}$ allele was included as an indirect reporter to identify Dre-recombined

141 cells, i.e., FOXO1 re-expression in *Foxo1*$^{stopRox}$ mice (Fig. 2C). Strikingly, TAM
142 administration with subsequent FOXO1 re-activation in the *Foxo1*$^{fl/stopRox}$ group
143 completely restored the DZ compartment in ZsGreen$^{+}$ GCBCs, up to the same levels as
144 in *Foxo1*$^{fl/wt}$ control mice (Fig. 2D). This observation also suggests a high efficiency of
145 Dre-mediated recombination in this setting, since all rox sites available (here the rox
146 sequences in *Foxo1*$^{stopRox}$ and *R26-ZsGreen*$^{stopRox}$ alleles) are targeted in the same cell.
147 In contrast, ZsGreen$^{-}$ GCBCs in the experimental *Foxo1*$^{fl/stopRox}$ group, which had failed
148 to recombine the *Foxo1*$^{stopRox}$ allele by Dre and had remained a full FOXO1-KO, lost the
149 physiological levels of the DZ/LZ ratio, at the expense of DZ cells (Fig. 2D) and in
150 agreement with previous studies[14,15]. Additionally, CSR to IgG1 was robustly restored in
151 ZsGreen$^{+}$ GCBCs in the *Foxo1*$^{fl/stopRox}$ group, albeit at a lower frequency compared to
152 controls (Fig. 2E). We attribute this lower level to the fact that reporter ZsGreen$^{+}$ cells
153 from the *Foxo1*$^{fl/stopRox}$ mice have resided in the GC only for a maximum of 4 days (after
154 TAM administration), in contrast to the control cells, which have participated in the GC
155 reaction from the beginning. This considerable rescue of class-switching in GCBCs at
156 the peak of the GC reaction suggests that CSR can robustly be induced during the GC
157 response, irrespective of its frequent occurrence at the pre-GCBC stage[13].

158 In summary, our newly established *Cγ1-CDE* allele allows for highly efficient Cre and
159 subsequent Dre recombination in the context of GCBCs. Thus, this tool can be used *in*
160 *vivo* not only to model the sequential acquisition of genetic alterations acquired during
161 malignant transformation but also to study the interplay of two or more genetic events or
162 the function of a specific gene at different time points during the GC reaction. A similar
163 strategy of sequential targeted mutagenesis could be applied in other cellular contexts.

164


165 1. Li, H., Weng, W. & Zhou, B. Perfect duet: Dual recombinases improve genetic resolution.
166 *Cell Prolif.* 56, 1–12 (2023).

167 2. Sket, T., Falcomatà, C. & Saur, D. Dual Recombinase–Based Mouse Models Help
168 Decipher Cancer Biology and Targets for Therapy. *Cancer Res.* 83, (2023).

169 3. Victora, G. D. & Nussenzweig, M. C. Germinal Centers. *Annu. Rev. Immunol.* 40, (2022).

170 4. Chi, X., Li, Y. & Qiu, X. V(D)J recombination, somatic hypermutation and class switch
171 recombination of immunoglobulins: mechanism and regulation. *Immunology* vol. 160,
172 (2020).

173 5. Küppers, R., Klein, U., Hansmann, M. L. & Rajewsky, K. Cellular origin of human B-cell
174 lymphomas. *N. Engl. J. Med.* (1999).

175 6. Casola, S. *et al.* Tracking germinal center B cells expressing germ-line immunoglobulin γ1
176 transcripts by conditional gene targeting. *Proc. Natl. Acad. Sci. U. S. A.* (2006).

177 7. Weber, T. *et al.* A novel allele for inducible Cre expression in germinal center B cells. *Eur.*
178 *J. Immunol.* (2019).

8. Dogan, I. *et al.* Multiple layers of B cell memory with different effector functions. *Nat. Immunol.* 10, (2009).

9. Shinnakasu, R. *et al.* Regulated selection of germinal-center cells into the memory B cell compartment. *Nat. Immunol.* (2016).

10. Callahan, D. *et al.* Memory B cell subsets have divergent developmental origins that are coupled to distinct imprinted epigenetic states. *Nat. Immunol.* (2024).

11. Sommermann, T. *et al.* Functional interplay of Epstein-Barr virus oncoproteins in a mouse model of B cell lymphomagenesis. *Proc. Natl. Acad. Sci. U. S. A.* 117, (2020).

12. Biglari, N. *et al.* Functionally distinct POMC-expressing neuron subpopulations in hypothalamus revealed by intersectional targeting. *Nat. Neurosci.* 24, (2021).

13. Roco, J. A. *et al.* Class-Switch Recombination Occurs Infrequently in Germinal Centers. *Immunity* (2019).

14. Dominguez-Sola, D. *et al.* The FOXO1 Transcription Factor Instructs the Germinal Center Dark Zone Program. *Immunity* 43, (2015).

15. Sander, S. *et al.* PI3 Kinase and FOXO1 Transcription Factor Activity Differentially Control B Cells in the Germinal Center Light and Dark Zones. *Immunity* 43, (2015).

16. Paik, J. H. *et al.* FoxOs Are Lineage-Restricted Redundant Tumor Suppressors and Regulate Endothelial Cell Homeostasis. *Cell* 128, (2007).

17. Hosaka, T. *et al.* Disruption of forkhead transcription factor (FOXO) family members in mice reveals their functional diversification. *Proc. Natl. Acad. Sci. U. S. A.* 101, (2004).

18. Furuyama, T. *et al.* Abnormal angiogenesis in Foxo1 (Fkhr)-deficient mice. *J. Biol. Chem.* 279, (2004).

Conflict of interest: The authors declare no conflict of interest.

Acknowledgements: We thank all members of the K. Rajewsky lab for discussion, R. Kühn (MDC transgenic facility), H.P. Rahn (MDC FACS facility), G. Natale (K. Rajewsky lab, MDC) for excellent technical support and the MDC animal caretakers for their outstanding technical help. Figure schematics were created using images from BioRender. This work was supported by the European Research Council (ERC Advanced Grant 268921) to K.R., the Deutsche Krebshilfe (grant #70112800) to K.R. and M.J., and the Berlin School of Integrative Oncology (BSIO) to C.F.D. We apologize to colleagues whose work could not be cited owing to space limitation.

Author contributions: C.F.D., E.K. and W.W. designed the experiments; C.F.D., E.K., W.W. and C.S. performed experiments; T.W. provided the *R26-ZsGreen*$^{stopRox}$ strain; C.F.D. and E.K. analyzed data and wrote the manuscript; M.J. and K.R. supervised all aspects of the study, and reviewed and edited the manuscript.

# FIGURE 1

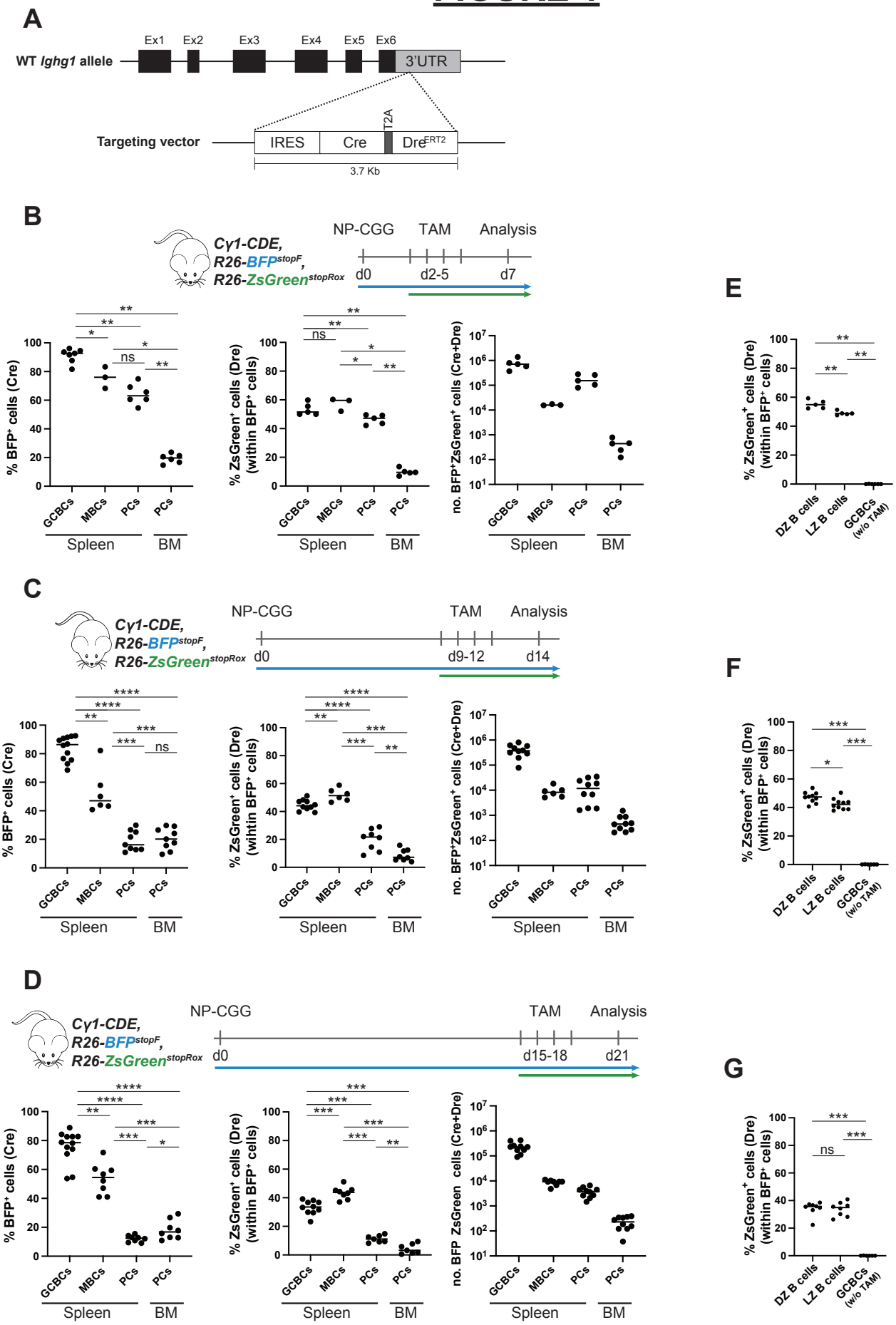
A
WT Ighg1 allele
Ex1
Ex2
Ex3
Ex4
Ex5
Ex6
3'UTR
Targeting vector
IRES
Cre
T2A
DreERT2
3.7 Kb
B
Cγ1-CDE,
R26-BFPstopF,
R26-ZsGreenstopRox
NP-CGG
TAM
Analysis
d0
d2-5
d7
% BFP+ cells (Cre)
% ZsGreen+ cells (Dre) (within BFP+ cells)
no. BFP+ZsGreen+ cells (Cre+Dre)
GCBCs
MBCs
PCs
PCs
Spleen
BM
C
Cγ1-CDE,
R26-BFPstopF,
R26-ZsGreenstopRox
NP-CGG
TAM
Analysis
d0
d9-12
d14
% BFP+ cells (Cre)
% ZsGreen+ cells (Dre) (within BFP+ cells)
no. BFP+ZsGreen+ cells (Cre+Dre)
GCBCs
MBCs
PCs
PCs
Spleen
BM
D
Cγ1-CDE,
R26-BFPstopF,
R26-ZsGreenstopRox
NP-CGG
TAM
Analysis
d0
d15-18
d21
% BFP+ cells (Cre)
% ZsGreen+ cells (Dre) (within BFP+ cells)
no. BFP ZsGreen cells (Cre+Dre)
GCBCs
MBCs
PCs
PCs
Spleen
BM
E
% ZsGreen+ cells (Dre) (within BFP+ cells)
DZ B cells
LZ B cells
GCBCs (w/o TAM)
F
% ZsGreen+ cells (Dre) (within BFP+ cells)
DZ B cells
LZ B cells
GCBCs (w/o TAM)
G
% ZsGreen+ cells (Dre) (within BFP+ cells)
DZ B cells
LZ B cells
GCBCs (w/o TAM)

**Figure 1. Characterization of the *Cγ1-CDE* strain.** (A) Targeting strategy for the insertion of the IRES-Cre_T2A_DreERT2 cassette into the 3'-UTR of the mouse *Cγ1* locus. (B-G) Experimental scheme using the *Cγ1-CDE, R26-BFP*$^{stopF}$*, R26-ZsGreen*$^{stopRox}$ compound mutant mice, immunizing with NP-CGG at day 0, administrating TAM at day 2-5 (B and E), 9-12 (C and F) or 15-18 (D and G) and analyzing at day 7, 14 or 21, respectively. (B-D) Percentage of Cre-mediated BFP$^{+}$ (left panel) and Dre-recombined ZsGreen$^{+}$ (within the BFP$^{+}$) cells (middle panel) among splenic Fas$^{+}$CD38$^{-}$ GCBCs, splenic Fas$^{-}$CD38$^{+}$IgD$^{-}$IgG1$^{+}$ MBCs and CD138$^{+}$TACI$^{+}$ PCs from spleen and BM (from one femur and tibia); as well as corresponding absolute numbers of the BFP$^{+}$ZsGreen$^{+}$ cells (right panel). (E-G) Percentage of ZsGreen$^{+}$ (within BFP$^{+}$) CXCR4$^{hi}$DC86$^{low}$ DZ and CXCR4$^{low}$CD86$^{hi}$ LZ GCBCs at day 7 (E), day 14 (F) and day 21 (G) after NP-CGG immunization. Data points for GCBCs without TAM administration are compiled from the three time points analyzed. Statistics: Mann-Whitney test *$P \leq 0.05$; **$P \leq 0.01$; ***$P \leq 0.001$; **** $P \leq 0.0001$; ns, not significant. Each dot represents one mouse. Data from at least two independent experiments. Horizontal lines indicate the median.

# FIGURE 2

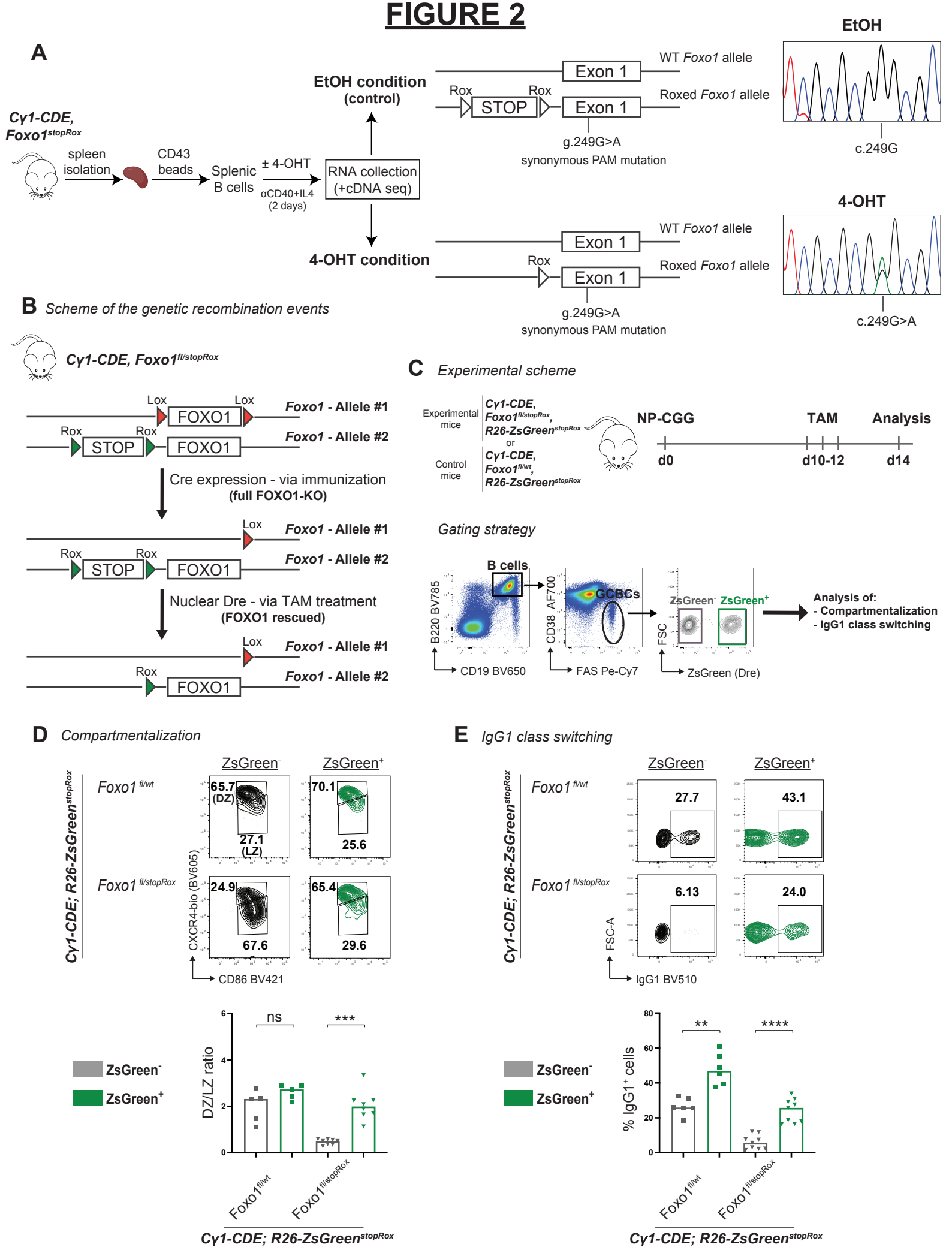
A
Cγ1-CDE, Foxo1stopRox
spleen isolation
CD43 beads
Splenic B cells
± 4-OHT
αCD40+IL4 (2 days)
RNA collection (+cDNA seq)
EtOH condition (control)
4-OHT condition
Exon 1
Rox
STOP
WT Foxo1 allele
Roxed Foxo1 allele
g.249G>A
synonymous PAM mutation
EtOH
4-OHT
c.249G
c.249G>A
B Scheme of the genetic recombination events
Cγ1-CDE, Foxo1fl/stopRox
Lox
FOXO1
Foxo1 - Allele #1
Foxo1 - Allele #2
Cre expression - via immunization
(full FOXO1-KO)
Nuclear Dre - via TAM treatment
(FOXO1 rescued)
C Experimental scheme
Experimental mice
Cγ1-CDE, Foxo1fl/stopRox, R26-ZsGreenstopRox
or
Control mice
Cγ1-CDE, Foxo1fl/wt, R26-ZsGreenstopRox
NP-CGG
TAM
Analysis
d0
d10-12
d14
Gating strategy
B cells
GCBCs
ZsGreen-
ZsGreen+
B220 BV785
CD19 BV650
CD38 AF700
FAS Pe-Cy7
FSC
ZsGreen (Dre)
Analysis of:
- Compartmentalization
- IgG1 class switching
D Compartmentalization
Cγ1-CDE; R26-ZsGreenstopRox
Foxo1 fl/wt
Foxo1 fl/stopRox
ZsGreen-
ZsGreen+
65.7 (DZ)
27.1 (LZ)
70.1
25.6
24.9
67.6
65.4
29.6
CXCR4-bio (BV605)
CD86 BV421
ns
***
DZ/LZ ratio
E IgG1 class switching
27.7
43.1
6.13
24.0
FSC-A
IgG1 BV510
**
****
% IgG1+ cells
Cγ1-CDE; R26-ZsGreenstopRox

248 **Figure 2**. **Sequential mutagenesis at the endogenous *Foxo1* locus.** (A) Schematic
249 representation of *in vitro* induction of the *Foxo1*$^{stopRox}$ allele by *Cγ1-CDE* (left) and cDNA
250 sequencing in activated *Cγ1-CDE, Foxo1*$^{stopRox}$ splenic B cells (right). Expression of the
251 targeted allele is observed only in the presence of 4-OHT, as demonstrated by the
252 detection of the synonymous PAM mutation introduced during the targeting strategy of
253 the transgenic strain. (B) Genetic scheme of recombination events after Cre and Dre
254 activation at the *Foxo1* locus of *Foxo1*$^{fl/stopRox}$ animals. (C) Experimental scheme (top)
255 and representative gating strategy (bottom) employed for the phenotypic analysis of the
256 GC compartment. (D-E) Top: Representative flow cytometry plots measuring the
257 percentage of DZ and LZ (D) and IgG1$^{+}$ (E) splenic GCBCs of mice of the indicated
258 genotypes at day 14 after immunization. Bottom: Quantification of the DZ/LZ ratio (D)
259 and the percentage of IgG1$^{+}$ (E) ZsGreen$^{-}$ (grey) and ZsGreen$^{+}$ (green) splenic GCBCs.
260 Statistics: Mann–Whitney test $^{**}P \leq 0.01$; $^{***}P \leq 0.001$; $^{****}P \leq 0.0001$; ns, not significant.
261 Each symbol represents one mouse. Data from three independent experiments.
262 Horizontal lines indicate the median.

263

264